A Prior-Form Distorted Wave Born Approximation Analysis of the Elastic Break-Up of 156 MeV ^{6}Li Projectiles

D. K. Srivastava, H. Rebel, N. Heide
Institut für Kernphysik

Kernforschungszentrum Karlsruhe

KERNFORSCHUNGSZENTRUM KARLSRUHE

Institut für Kernphysik

KfK 4565

A PRIOR-FORM DISTORTED WAVE BORN APPROXIMATION ANALYSIS OF THE ELASTIC BREAK-UP OF 156 MEV 6Li PROJECTILES

D.K. Srivastava*, H. Rebel, and N. Heide

*Variable Energy Cyclotron Centre, Bhabha Atomic Research Centre
Bidhan Nagar, Calcutta 700064, India

Abstract

Features of the prior-form distorted wave Born approximation theory of elastic break-up of 156 MeV [6]Li ions scattered off [208]Pb are investigated. Nuclear break-up for large relative energies of the outgoing α-particle and deuteron fragments ($E_{\alpha d} > 5$ MeV) studied here is found to proceed dominantly via the quadrupole scattering state of the α+d system when transition potentials from elastic fragment-target scattering are used for the calculations. The coherent contributions of different multipole components to the triple differential cross-sections appear to be very sensitive to the potentials generating the distorted waves and representing the cluster fragment-target interactions. The results of the analysis of the experimental data require transition potentials rather different from the on-the-mass shell optical potentials deduced from elastic α-particle and deuteron scattering.

ANALYSE DES ELASTISCHEN AUFBRUCHS VON 156 MEV
[6]Li PROJEKTILEN MIT DER PRIOR–FORM DWBA AUFBRUCHTHEORIE

Die Prior-Form DWBA Aufbruchtheorie wird für den Fall des elastischen Aufbruchs von 156 MeV [6]Li Projektilen untersucht. Für größere Relativenergien ($E_{\alpha d} > 5$ MeV) der α-Teilchen- und Deuteron-Fragmente dominiert die Quadrupolkomponente des nuklearen Aufbruchs, falls man als Übergangspotentiale die optischen Potentiale der elastischen Fragment-Target-Streuung für die Rechnungen zugrunde legt. Die kohärenten Beiträge verschiedener Multipolkomponenten des α+d Streusystems sind empfindlich auf die Potentiale, welche die "distorted waves" generieren und die Clusterfragment- Targetwechselwirkung beschreiben. Die Resultate der Analyse der experimentellen Wirkungsquerschnitte verlangen Übergangspotentiale, die sich erheblich von den optischen Potentialen unterscheiden, welche die elastische Streuung von α-Teilchen und Deuteronen wiedergeben.

CONTENT

1. INTRODUCTION

Theoretical studies of the break-up of light-ion projectiles in the nuclear and Coulomb field of nuclei have been enlivened by debates [1,2] on various ways and approximations in formulating correct theoretical descriptions of the break-up process. One problem concerns the validity and merits of the so-called post[3]- and prior[4]-form of distorted wave Born approximation theories for this type of nuclear reactions. The debate on this has its origin in the failure of the prior-form theory of Rybicki and Austern [4] in explaining the experimentally observed cross sections of the break-up of deuterons while the post-form theory of Baur et al [3] proves to be much more sucessful, in general. On the other hand, the theoretical formulation of the post-form has been criticized [5] because of numerical difficulties encountered in actual applications. In addition, though a finite-range development is feasible in an approximate way [6], the theory of Baur et al [3] uses a zero-range approximation which may obscure important features of the break-up process, in particular for light ions with Z > 2. In this respect, the prevailing formulation of the prior-form appears to be more suitable to carry out full finite-range calculations. The two alternative formulations of the DWBA break-up theory differ by different prescriptions for the three-body exit channel, first introduced by Henley and Lacy [7] and realized in different decompositions into an unperturbed and a perturbation part of the Hamiltonian

$$H = T_b + T_x + U_{bA}(\mathbf{r}_b) + U_{xA}(\mathbf{r}_x) + U_{bx}(\mathbf{r})$$ (1.1)

of the (elastic) break-up process

$$a + A \rightarrow b + x + A \ .$$ (1.2)

Here T_b and T_x denote the kinetic energies, U_{bA}, U_{xA} the interactions of the break-up fragments with target (A), and U_{bx} the interaction binding b and x in the projectile a with the ground state wave function $\phi_a(\mathbf{r})$. The neglect of the interaction U_{bx} in the final states leads to the currently used post-form DWBA formulation

$$T_{fi}^{post} = <\chi_b^{(-)} \chi_x^{(-)} | U_{bx} | \chi_a^{(+)} \phi_a>$$ (1.3)

with $\chi_a^{(+)}(\mathbf{R})$, $\chi_b^{(-)}(\mathbf{r}_b)$ and $\chi_x^{(-)}(\mathbf{r}_x)$ describing the motion of the particles under the influence of the potentials in the entrance and the exit channels, respectively. The prior-form T matrix equivalent to eq. (1.3) has been evaluated by Srivastava and Rebel [8] using a plane wave expansion of the distorted waves. In contrast, the prevailing form of the prior-form DWBA theory [4] includes the final state interaction to all orders by virtue of the explicit use of the continuum relative wave function $\phi_k^{(-)}$, while the nuclear break-up perturbation is associated to $U_{bA} + U_{xA}$ with the amplitude

$$T_{fi}^{prior} = < \chi_{a*}^{(-)} \, \phi_k^{(-)} \,|\, U_{bA} + U_{xA} \,|\, \chi_a^{(+)} \, \phi_a > \qquad (1.4)$$

In the present work we scrutinize the prior-form DWBA approach by an application to the analysis of recently measured [9-11] triple differential cross sections for the *elastic* break-up of 156 MeV ^{6}Li projectiles colliding with ^{208}Pb. These data are measured at large relative emission angles of the outgoing α-particle and deuteron fragments, thus selecting larger relative momenta k and larger momentum transfer Q of the reaction. Unlike the cross sections usually observed at smaller momentum transfer showing the familiar bell-shaped distributions of the fragments around the beam-velocity energies, these particular experimental coincidence cross sections exhibit conspicuously structured distributions, rapidly changing with the relative emission angles. First analyses [9-11] of the data within the DWBA and the diffractive dissociation approach [12] reveal considerable sensitivities to the actual ingredients of the calculations, i.e. the scattering potentials and scattering amplitudes, respectively as well as to the assumptions on the internal momentum distribution $| \tilde{\phi}_a |^2$. We use these features of the elastic ^{6}Li break-up data to explore the merits and deficiencies of the prior-form DWBA approach when using it for a quantitative description of nuclear break-up of light ions.

2. THEORETICAL BASIS

Writing the prior-form transition matrix (eq. 1.4) as

$$T_{fi}^{prior} = < \chi_{a*}^{(-)} (K_f, R) \,|\, F^{(N)} (k, R) \,|\, \chi_a^{(+)} (K_i, R) > \qquad (2.1)$$

with

$$F^{(N)} = < \phi_{a*}^{(-)} (k, r) \,|\, U_{bA} (R - \frac{m_x}{m_a} r) + U_{xA} (R + \frac{m_b}{m_a} r) \,|\, \phi_a(r) > \qquad , \qquad (2.2)$$

$$K_f = k_b + k_x \quad and \quad k = \frac{m_b}{m_a} k_x - \frac{m_x}{m_a} k_b \qquad (2.3)$$

we explicitly neglect the contribution of Coulomb excitation which is expected to be small at larger relative momenta k under consideration [13]. This also implies that the Coulomb-nuclear interference [4] may be feeble for ^{6}Li break-up and does not noticeably alter the shape of the cross sections.

The form factor (eq. 2.2) may be expanded in multipoles

$$F^{(N)} (k, R) = \sum_{\ell m} i^{-\ell} \, Y_{lm}^* (\hat{R}) \cdot \, Y_{\ell m} (\hat{k}) \, F_\ell (k, R) \quad . \qquad (2.4)$$

Similarily, we expand the scattering state

$$\phi_{a*}^{(-)} (k, r) = 4\pi \sum_{\ell m} i^\ell \, \phi_\ell (k r) \cdot \, Y_{\ell m} (\hat{k}) \cdot \, Y_{\ell m}^* (\hat{r}) \qquad (2.5)$$

with

$$\phi_\ell (k\,r) = u_\ell (k\,r) \,/\, k\,r \qquad (2.6)$$

To ensure orthogonality the scattering state $\phi_{a*}^{(-)}$ is generated by the same potential well as for the $\ell = 0$ ground state wave function of the relative a-particle - deuteron motion

$$\phi_a (\mathbf{r}) = \frac{u_0(r)}{r} \, Y_{00} (\hat{\mathbf{r}}) \qquad (2.7)$$

Introducing the Fourier transforms of the scattering potentials U_{bA} and U_{xA}

$$U_b (q) = \int_0^\infty dr \, r \sin qr \, U_{bA} (r) \qquad (2.8a)$$

$$U_x (q) = \int_0^\infty dr \, r \sin qr \, U_{xA} (r) \qquad (2.8b)$$

and with

$$v_\ell \left(k, \frac{m_i}{m_a} q \right) = q \int r^2 dr \, \phi_\ell (kr) j_\ell \left(\frac{m_i}{m_a} q \, r \right) \phi_a(r) \qquad (2.9)$$

($i = b, x$ and j_ℓ = spherical Bessel function)

the multipole component F_ℓ of the form factor is written

$$F_\ell (k, R) = 32 \, \pi \int_0^\infty dq \left[U_b (q) v_\ell \left(k, \frac{m_x}{m_a} q \right) \right.$$

$$\left. + (-1)^\ell U_x (q) v_\ell \left(k, \frac{m_b}{m_a} q \right) \right] \cdot j_\ell (qR) \qquad (2.10)$$

Correspondingly, the multipole expansion of the distorted waves $\chi_{a*}^{(-)}$ and $\chi_a^{(+)}$ is introduced, e.g.

$$\chi^{(+)} (\mathbf{K}, \mathbf{R}) = \frac{4\pi}{KR} \sum_{LM} i^L (2L+1) \chi_L (K, R) Y_{LM}^* (\hat{\mathbf{R}}) \cdot Y_{LM} (\hat{\mathbf{K}}) \qquad (2.11)$$

defining the radial matrix elements

$$f_{L_f L_i}^\ell = \frac{K_f}{K_i} \int_0^\infty dR \, \chi_{L_f} (K_f, R) F_\ell (k, R) \chi_{L_i} (K_i, R) \qquad (2.12)$$

With the angular momentum coefficients

$$\Gamma_{L_f L_i}^{\ell m} = i^{L_i - L_f - \ell} (2L_f + 1) \left[\frac{(L_f - m)!}{(L_f + m)!} \right]^{1/2}$$

$$< L_f \, \ell \, 0 \, 0 | L_i \, 0 > \, < L_f \, \ell \, m \, - m | L_i \, 0 > \qquad (2.13)$$

and the standard DWBA matrix elements

$$\beta_{lm}^{(N)} = \sum_{L_f L_i} \Gamma_{L_f L_i}^{\ell m} f_{L_f L_i}^{\ell} P_{L_f}^m (\cos \theta_f) \qquad (2.14)$$

the transition amplitude is given by

$$T_{fi}^{prior} = \sum_{\ell} T_{\ell}^{(N)} \qquad (2.15a)$$

where

$$T_{\ell}^{(N)} = [4\pi(2\ell+1)]^{1/2} K_f^{-2} \sum_{m} Y_{\ell m}(\hat{k}) \beta_{\ell m}^{(N)} \quad . \qquad (2.15b)$$

Alternatively, we may identically rewrite

$$T_{fi}^{prior} = \frac{\sqrt{4\pi}}{K_i K_f} \sum_{\ell m L_f} \sqrt{2\ell+1} \; Y_{\ell m}^{*}(\hat{k}) \, Y_{L_f m}(\hat{K}_f) \, a_{L_f}^{(N) \, \ell m} \qquad (2.16)$$

with

$$a_{L_f}^{(N) \, lm} = (-1)^m \left(\frac{4\pi}{2L_f+1} \right)^{1/2} \left[\frac{(L_f+m)!}{(L_f-m)!} \right]^{1/2} \left(\frac{K_i}{K_f} \right) \sum_{L_i} \Gamma_{L_f L_i}^{\ell m} f_{L_f L_i}^{\ell} \quad . \qquad (2.17)$$

The representation of T_{fi}^{prior} by eqs. (2.16 - 2.17) is useful when stuying the localisation of the reaction in the angular momentum space (L_f) and for the discussion of possible interferences of different multipoles.

The triple differential cross section for scattering the centre-of-mass of the fragmented projectile into the solid angle $d\Omega$ with the relative motion vector pointing into the direction $d\Omega_{rel}$ and with the relative energy of the fragments between E_{bx} and $E_{bx} + dE_{bx}$ is given by

$$\frac{d^3\sigma}{d\Omega d\Omega_{rel} dE_{bx}} = \frac{2\pi}{\hbar v} \, | T_{fi}^{prior} |^2 \, \rho_{phase} = \frac{\mu_{bx} \mu_a^2}{(2\pi)^5 \hbar^6} \frac{K_f}{K_i} k \, | T_{fi}^{prior} |^2 \quad . \qquad (2.18)$$

There

$$\mu_{bx} = \frac{m_b \, m_x}{m_b + m_x} \quad , \quad \mu_a = \frac{m_a \, m_A}{m_a + m_A} \qquad (2.19)$$

and

$$E_{bx} = \frac{\hbar^2 k^2}{2\mu_{bx}} \quad . \qquad (2.20)$$

By virtue of the representation through eq. (2.16) the angle integrated cross section

$$\frac{d\sigma}{dE_{bx}} = \frac{2\pi}{\hbar v} \cdot \rho_{phase} \cdot \int | T_{fi}^{prior} |^2 \, d\Omega \, d\Omega_{rel} \qquad (2.21)$$

can be decomposed into

$$\frac{d\sigma}{dE_{bx}} = \sum_{\ell, L_f} \sigma_\ell^{(N)}(L_f, E_{bx}) \qquad (2.22)$$

with

$$\sigma_\ell^{(N)}(L_f, E_{bx}) = \frac{2\pi}{\hbar \upsilon} \, \rho_{phase} \, \frac{4\pi(2\ell+1)}{K_i^2 K_f^2} \sum_m |a_{L_f}^{(N)\ell m}|^2 \quad . \qquad (2.23)$$

On the other hand the triple differential cross section for elastic break-up in the laboratory system is given by

$$\frac{d^3\sigma}{d\Omega_b^L \, d\Omega_x^L \, dE_b^L} = \frac{m_b \, m_a}{(2\pi)^5 \hbar^7} \cdot \frac{p_b^L}{p_a^L} \, | \, T_{fi}^{prior} \, |^2 \cdot \, phase \, factor \qquad (2.24)$$

$$phase \, factor = \frac{m_x \, m_A \, p_x^L}{(m_b + m_A) + (m_x (\mathbf{p}_b^L - \mathbf{p}_a^L) \cdot \, \mathbf{p}_x^L)/(p_x^L)^2} \qquad (2.25)$$

where p_i^L and m_i are the laboratory momenta and the masses of the particles $i = a, b, x$. The numerical integration over dE_b^L yields the angular correlation.

3. GENERAL FEATURES OF THE T-MATRIX

We apply the theoretical formulation of the prior-form T-matrix to the calculations of elastic break-up of 156 MeV ^{6}Li projectiles incident on ^{208}Pb in a typical kinematical situation where the coincidently emitted α-particle and deuteron fragments are detected at $\theta_\alpha = 10°$ and $\theta_d = -10°$, on different sides of the beam-axis. The distorted waves for the ^{6}Li and the α-d center - of - mass motion are generated by the elastic scattering potentials [14], and also the interaction potentials $U_{\alpha Pb}$ and U_{dPb} are identified with potentials deduced from (on-shell) elastic scattering [15,16] according to the present convention[17,18]. Tabs. 1 - 2 compile the potentials used for the DWBA and form factor calculations.

Fig. 1 displays the real and imaginary parts of various multipole components of the form factor $F^{(N)}(k, R)$ for the case when the α-particle is emitted with the beam-velocity energy of 104 MeV. This corresponds to a relative energy $E_{\alpha d} = 4.4$ MeV or $k = 0.51$ fm^{-1} for the elastic break-up.

Due to the strong oscillations of the monopole and dipole form factors within the range of the nuclear interaction their contributions are expected to be smaller than that of the dominant quadrupole component (the real part of) which does not alter sign beyond $R \simeq 3$fm. The octupole mode (and modes of higher multipolarities) are additionally present in the surface region, but with significantly smaller contributions. Inspecting the shapes of the form factors it is

Tab. 1   Saxon-Woods form optical potentials for the ^{6}Li + ^{208}Pb scattering (from ref. 14).

V_0 [MeV]	r_{0v} [fm]	a_v [fm]	W_0 [MeV]	r_{0w} [fm]	a_w [fm]	Remark
-240.0	1.17	0.766	-20.0	1.55	1.015	Set I
-113.5	1.3	0.673	-16.2	1.70	0.995	Set II

Tab. 2   Fragment - ^{208}Pb interaction and α-particle-deuteron potentials (Saxon-Woods form).

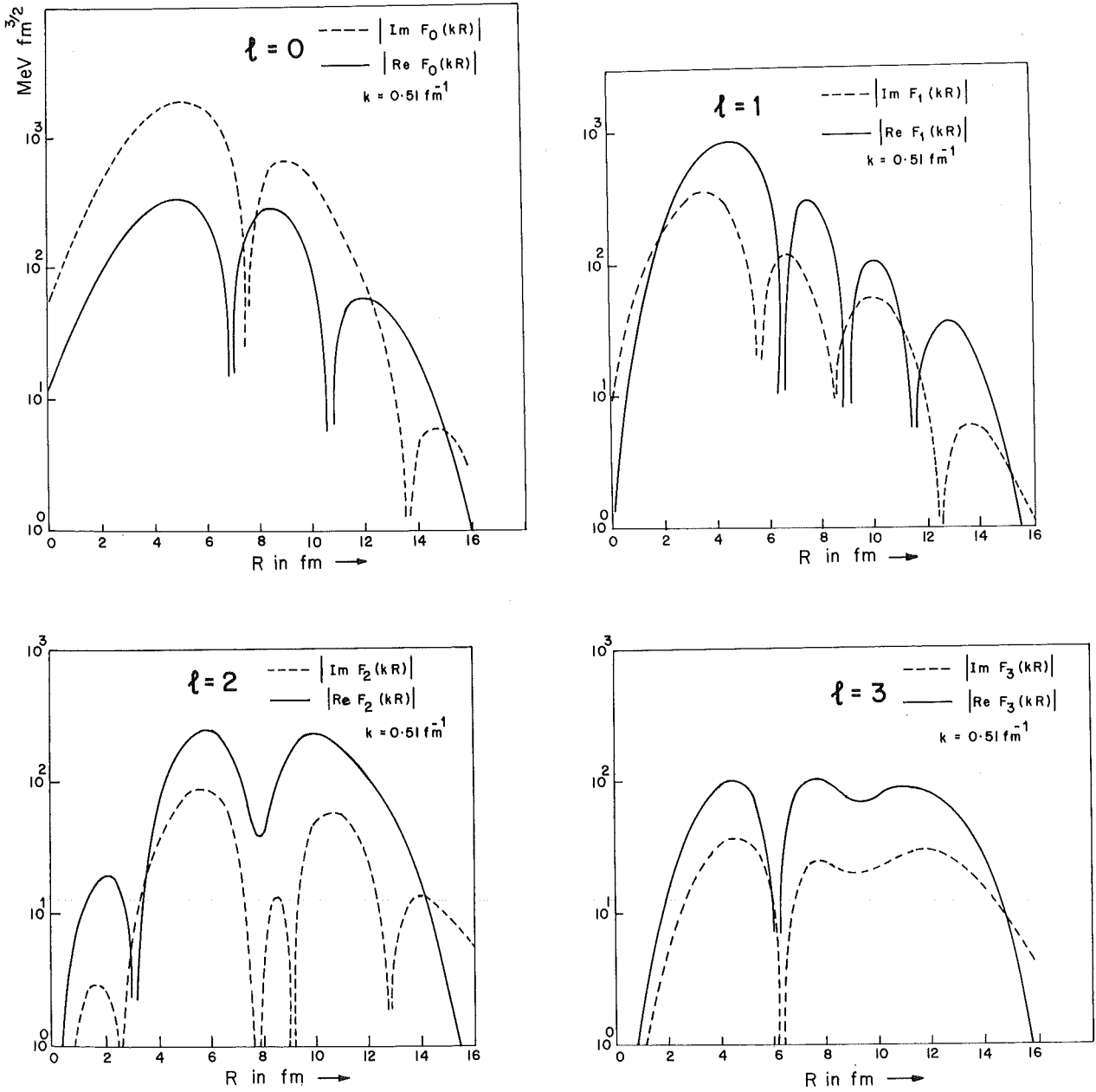| V_0 [MeV]	r_{0v} [fm]	a_v [fm]	W_0 [MeV]	r_{0w} [fm]	a_w [fm]	$J_v / A_p A_T$ [MeV $\cdot$ fm^3]	Remark
-146.0	1.222	0.830	-17.6	1.565	0.830	315	$U_{\alpha Pb}$ (ref. 15)
-90.5	1.150	0.755	-9.0	1.630	0.626	333	$U_{\alpha Pb}$ (ref. 16)
-83.5	1.42	0.70	–	–	–	-	$U_{\alpha d}$ (ref. 13)

Fig. 1 Real and imaginary parts of various multipoles of the nuclear form factor for elastic break-up of 156 MeV ^{6}Li scattered of ^{208}Pb. The value of the relative momentum k of the α-particle and deuteron fragments corresponds to $E_\alpha^L = 104$ MeV, $\theta_\alpha = 10°$ and $\theta_d = -10°$.

obvious that they can hardly be approximated, say by a derivative of a Saxon-Woods form. However, the radial shapes of the form factors of all multipolarities are similar beyond R ≃ 14 fm and may be represented [1] by any of the rapidly decreasing surface interactions used in nuclear physics studies.

The relative importance of various multipole components in nuclear break-up of ^{6}Li is evident in fig. 2 showing the angular correlation for the above kinematic condition. For the conventional transition potentials the calculations used set I of tab. 1 for generating the distorted waves. The feature that in the case of ^{6}Li break-up monopole and dipole terms contribute very little is in contrast to the finding with the break-up of the deuteron [4,17] and ^{3}He [18] (proceeding mainly via $\ell = 1$).
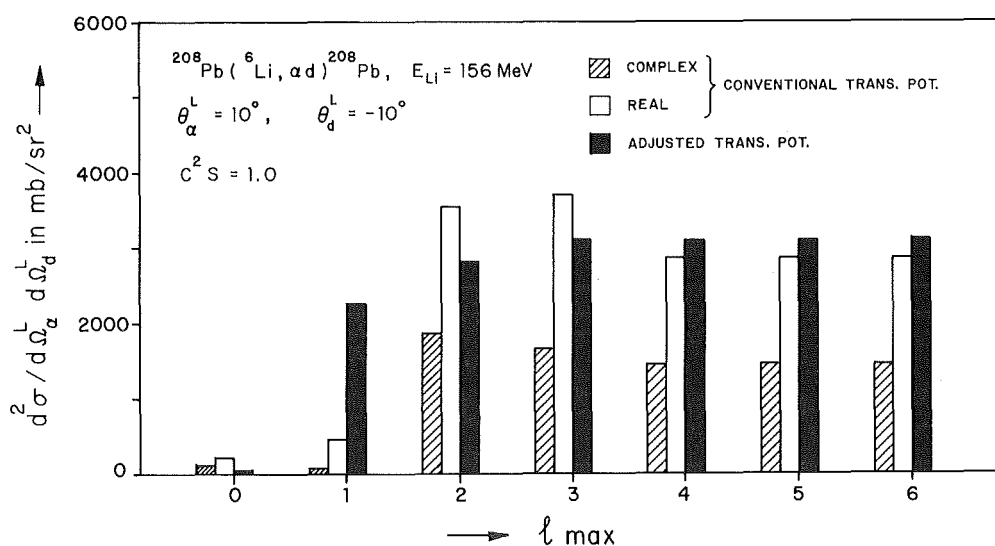

Fig. 2   Angular correlation for the kinematic situation given in fig. 1 using real and complex transition potentials. In addition to the conventional potentials (tab. 2), results for the adjusted potentials (to be described later) are given for comparison; ℓ_{max} denotes the maximum multipolarity taken into account.

Angular correlation (fig. 2) and triple differential cross sections (fig. 3) display how real and complex form factors (deduced from the potentials given in tab. 2) affect the magnitude of the cross sections. Fig. 3 also reveals that sufficient convergence is achieved by including contributions up to $\ell = 4$. However, one may argue that in elastic break-up, with both fragments escaping from the target
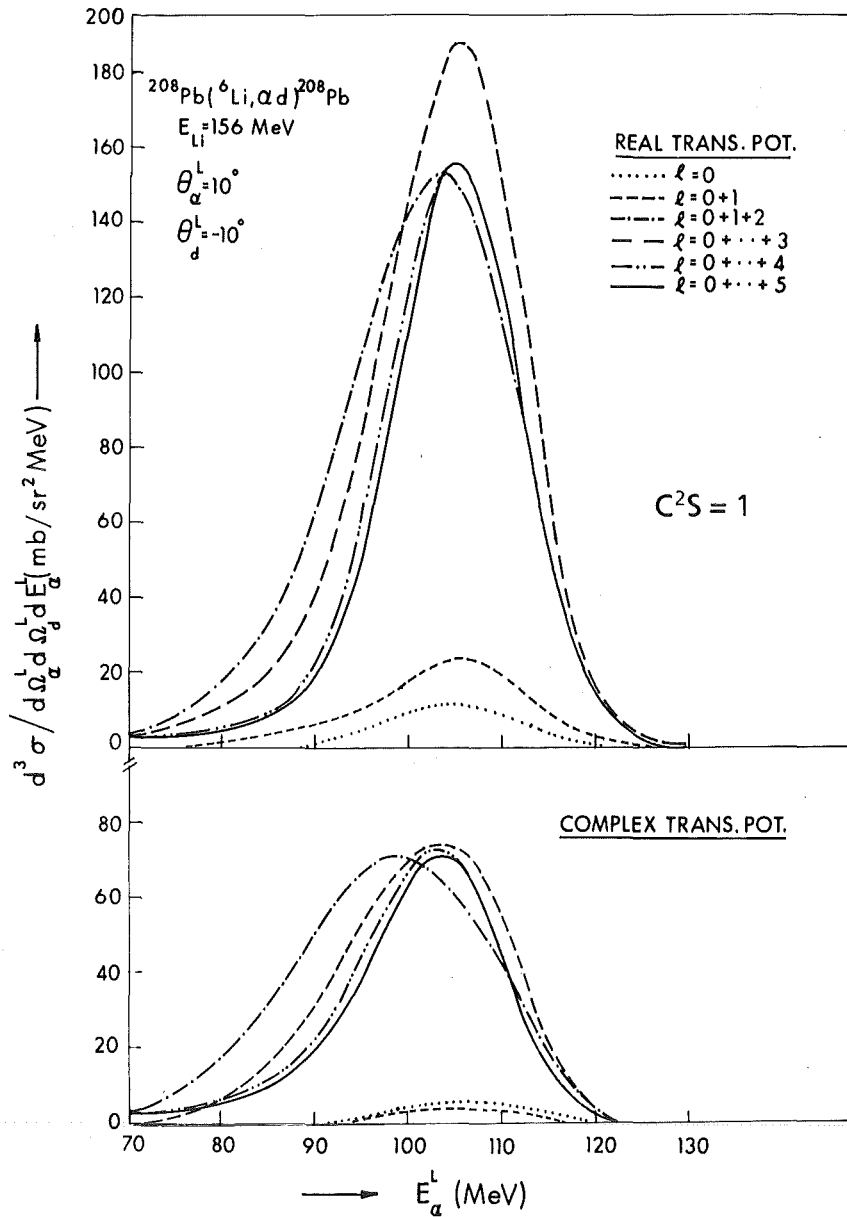
Fig. 3   Calculated triple differential cross section for elastic break-
up of 156 MeV ^{6}Li colliding with ^{208}Pb, resulting from
transition potentials deduced from elastic scattering of the
fragments.

nucleus, the absorption of α-particles and deuterons appears to be already taken
into account by the removal of ^{6}Li from the incident flux, and thus the use of real
transition potentials may be preferable for these studies. The exit and entrance
channel distorting potentials should, however, also take the effects of the

dynamic polarization potential[19,20] due to the break-up channels properly into account.

The surface localization of elastic break-up of ^{6}Li is brought out by fig. 4 showing $|a_{L_f}^{(N)\,\ell m}|^2$ vs the exit channel angular momentum L_f for various multipolarities (ℓ, m). For $m = 0$ all $|a_{L_f}^{(N)\,\ell m}|^2$ coefficients have a double-peaked structure with maxima at $L_f \simeq 34$ (only seen for $\ell = 1$ in fig. 4) and $L_f \simeq 60$ with a dip at $L_f \simeq 47$. The larger L_f peak is located a little below the angular momentum value $(L_g = 68)$ of the grazing partial wave. This implies that the break-up
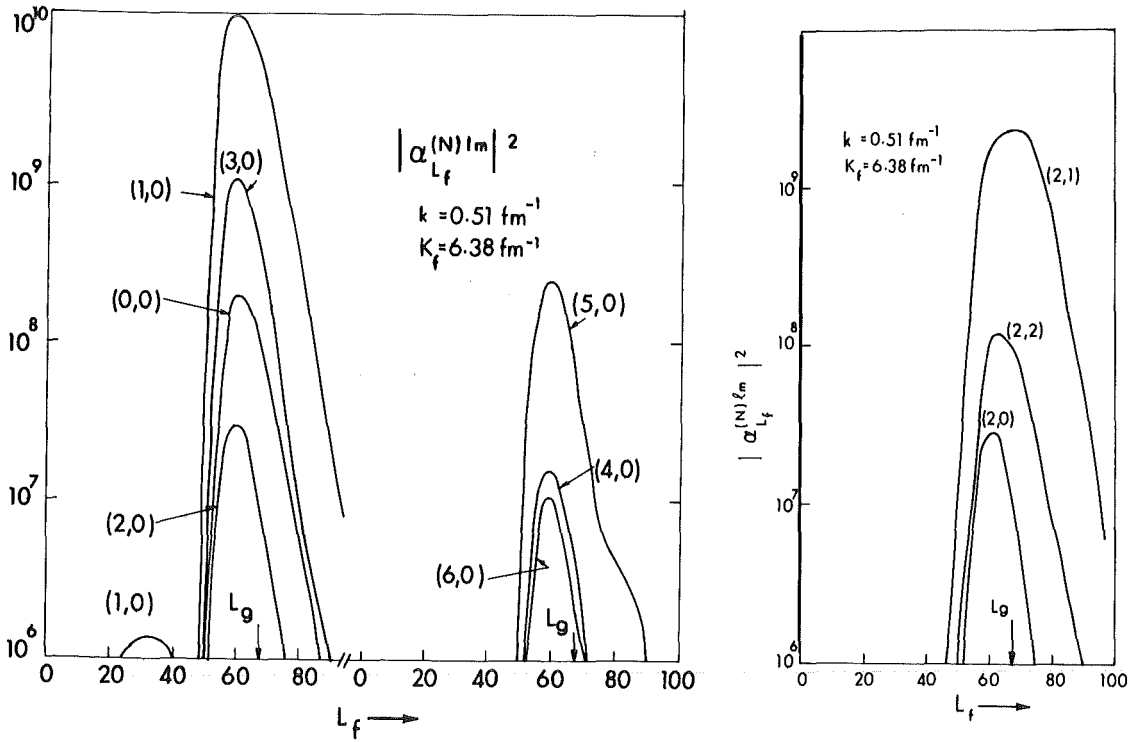

Fig. 4   Squared nuclear break-up matrix elements $|a_{L_f}^{(N)\,\ell m}|^2$ for different (ℓ, m) values as function of the exit channel angular momentum L_f for the kinematic condition of fig. 1. The grazing angular momentum is indicated by L_g, and conventional transition potentials have been used.

predominantly happens in a peripheral region ca. 1.2 fm inside the so-called strong absorption radius. For a more quantitative understanding of this aspect tab. 3 compiles the values of maxima of the $|a_{L_f}^{(N)\,\ell m}|^2$ coefficients. The outer peak exceeds the inner peak by ca. 4 orders of magnitudes. This is different from the

Tab. 3　The peak values of $|\alpha_{L_f}^{\ell m}|^2$ for nuclear break-up of 156 MeV ^{6}Li incident on ^{208}Pb at the smaller angular momentum ($L_f \simeq 34$) compared to that at the larger angular momentum ($L_f \simeq 60$).

ℓ	m	L_f	$|\alpha_{L_f}^{\ell m}|^2$	L_f	$|\alpha_{L_f}^{\ell m}|^2$
0	0	33	$2.15 \cdot 10^4$	60	$2.01 \cdot 10^8$
1	0	33	$1.38 \cdot 10^6$	60	$1.30 \cdot 10^{10}$
2	0	34	$4.49 \cdot 10^3$	59	$2.97 \cdot 10^7$
3	0	34	$1.51 \cdot 10^5$	60	$1.08 \cdot 10^9$
4	0	34	$2.43 \cdot 10^3$	59	$1.54 \cdot 10^7$
5	0	34	$3.81 \cdot 10^4$	59	$2.44 \cdot 10^8$
6	0	34	$1.68 \cdot 10^3$	59	$1.06 \cdot 10^7$

These results correspond to the case $\theta_\alpha = 10°$, $\theta_d = -10°$ and $E_\alpha = 104$ MeV.

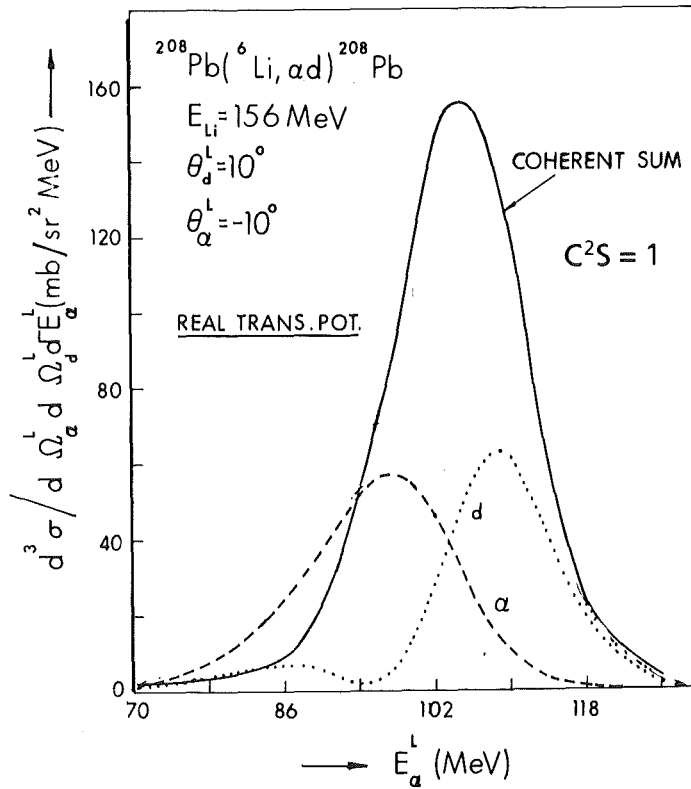Set I of the optical potential and complex transition potentials from tab. 2 are used.

Fig. 5   Contribution of the α-particle and deuteron scattering to the triple differential cross section for the nuclear break-up of 156 MeV 6Li projectiles colliding with 208Pb.
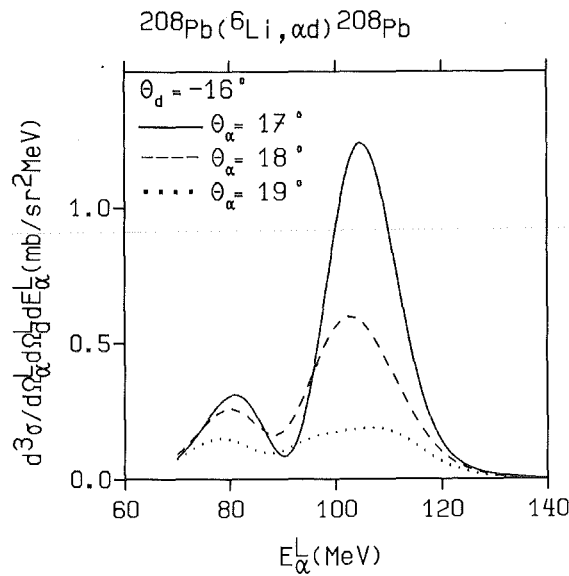

Fig. 6   Theoretical cross sections for elastic 6Li break-up at E_{Li} = 156 MeV using interaction potentials $U_{\alpha Pb}$ and U_{dPb} deduced from elastic scattering (tab. 2).

cases of deuterons [17] and ^{3}He [18] where the ratio of the inner to the surface contributions is less extreme. The smooth behaviour of the coefficients as function of L_f in the surface region suggests a parametrization by a convenient phenomenological form [1].
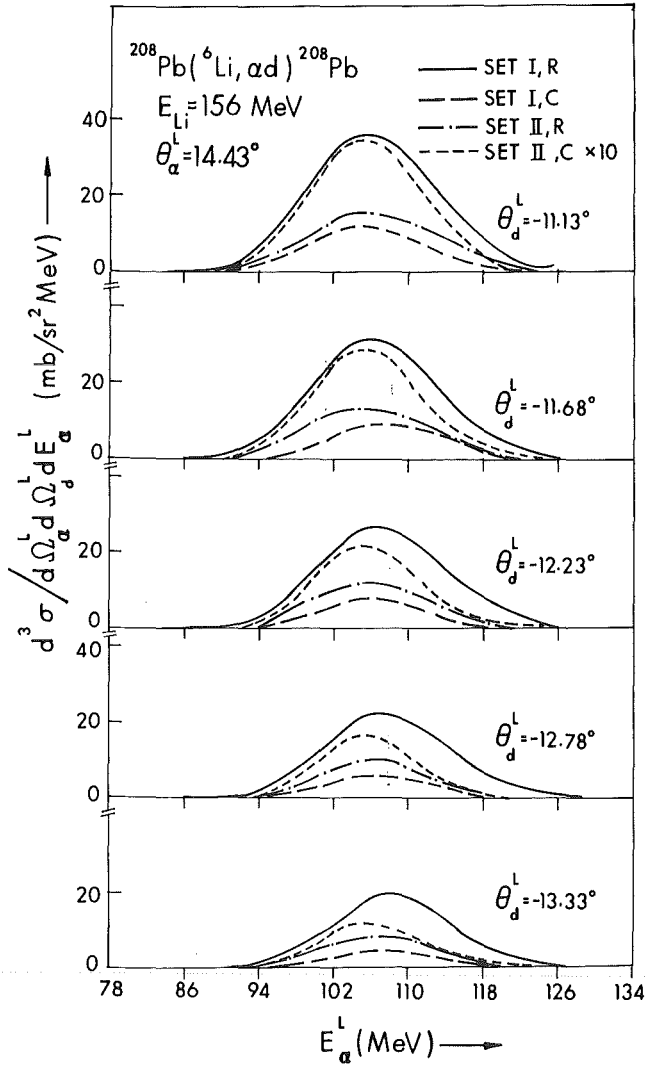

Fig. 7
Sensitivity of the prior-form DWBA cross sections to the optical potentials (tab. 1) generating the distorted waves and to the real (R) and complex (C) transition potentials (tab. 2).

Since for elastic break-up the transition matrix (eq. 2.1) and the form factor (eq. 2.2), respectively, can be split in two parts corresponding to the two off-shell scattered fragments, there exists an interference of the two partial amplitudes of

$$T_{fi}^{prior} = T_b + T_x \tag{3.1}$$

which generally affects the shapes of the cross sections (see ref. 10). This is demonstrated in fig. 5 showing the different contributions to the triple differential cross section.

In case of real transition potentials the two contributions are of the same order. They add up destructively for $E_\alpha^L < 94$ MeV and interfere constructively for large α-particle energies. The situation is somewhat different for complex transition potentials. These features may lead to specific interference patterns [9-11] depending on the particular kinematic situation, further enriched when either of the off-shell scattering T - matrices of the fragments pass through minima across the fragment-energy range covered by the data. Fig. 6 gives an example where the theory predicts quite unfamiliar double peaked structured shapes of the triple differential cross sections, actually observed in a particular range of momentum
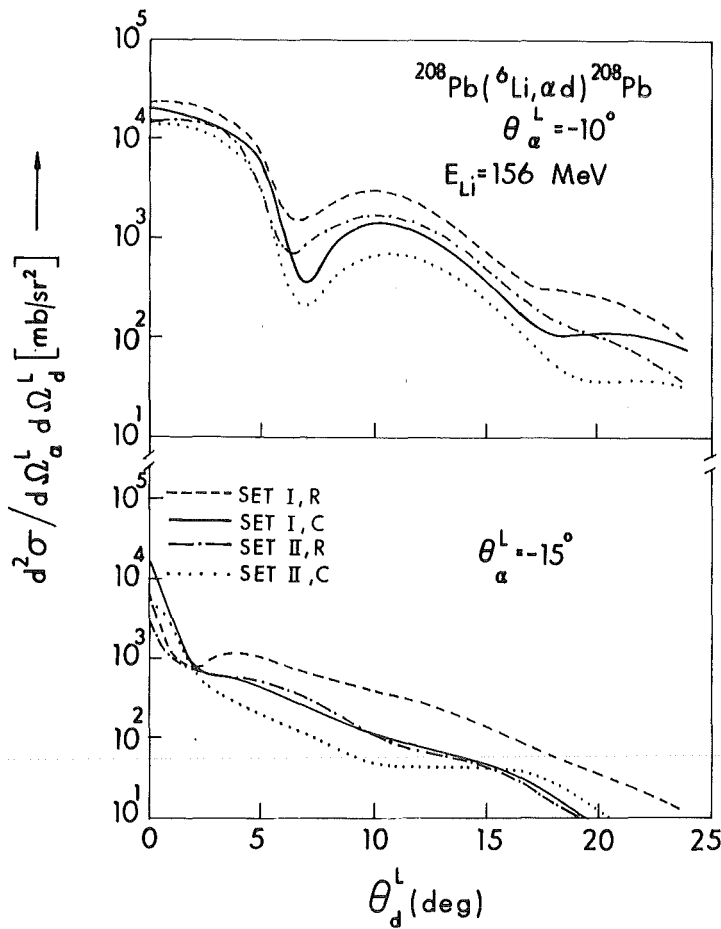

Fig. 8   Sensitivity of the theoretically predicted angular correlation to the optical potentials (tab. 1) generating the distorted waves and to the real (R) and complex (C) transition potentials (tab. 2).

transfer of the 6Li break-up reaction. Such effects call the quasi-free break-up model [21] into question as it takes into account only one of the terms in eq. (3.1), depending on the kinematic condition.

A crucial question of reliable theoretical predictions on the basis of the prior-form DWBA approach is the problem of optical potentials generating the distorted waves, in particular in the exit channel describing the center-of-mass motion of the fragments. The present application uses the entrance channel optical potentials for the exit channel, too. The dependence on the specific choice of the potential is examined in fig. 7 and 8 by calculations of the triple differential cross sections and angular correlations, respectively, using the two sets of parameters of tab. 1. The results indicate that the elastic break-up of ^{6}Li at higher incident energies is rather sensitive to details of all potentials involved. This along with the interference effects discussed above may provide an accurate handle [9,10] to study the off-shell behaviour of the nuclear interactions *if the wave functions are known*.

4. ANALYSIS OF EXPERIMENTAL TRIPLE DIFFERENTIAL CROSS SECTIONS

The study of the general features of prior-form DWBA T-matrix in the preceding chapter has revealed various sensitivities of the calculated cross sections to the ingredients of the theory, in particular to the specific choice of the optical potentials generating the distorted waves and of the cluster target-nucleus interactions inducing the break-up transition. However, identifying the break-up interactions with the optical potentials (or the real parts) which describe the (on-the-mass-shell) elastic scattering of the fragments (as $U_{\alpha Pb}$ and U_{dPb} of tab. 2 do) has no fundamental ground. On the contrary, the off-shell transition potentials (possibly affected by the presence of a third particle, the "reaction spectator") may significantly differ in strength and shape. In the present analysis of elastic break-up of 156 MeV ^{6}Li ions incident on ^{208}Pb we take the view to determine these transition potentials phenomenologically (within the constraint of a Saxon-Woods functional form) by adjustments to the data. Unlike the triple differential cross sections observed for smaller relative energies of the outgoing fragments, the experimental results under consideration here [11] show conspicuous structures, strongly varying with the relative momenta k of the outgoing fragments and the momentum transfer Q. These features may also help to reduce uncertainties due to other ingredients. The analysis is based on the following assumptions :

(i) The ground state ϕ_a and the scattering states $\phi_{a*}^{(-)}$ generated by the real "bound-state" potential given in tab. 2 and sucessfully used in other studies [13] are "correct" and not at disposal, even if the if the manner in which the internal momentum distribution manifests itself may be

considered as an aspect of its own interest [22]. Considering the peripheral nature of elastic break-up reactions this assumption will not be severe.

(ii) Distorted waves generated by set I of the optical potential (tab. 1) describing 6Li - 208Pb elastic scattering represent correctly the entrance *and* exit channel c. o. m. motion.

Nevertheless we have also to recall Austern's findings [5] of unusual potentials for the exit channel distortion. We feel that these effects can be approximately absorbed[10] by appropriate transition potentials.

(iii) The transition potentials are real

Additionally to the arguments given above, the results of the theoretical calculations of the triple differential cross sections for elastic 6Li break-up, when the fragments are emitted with $\theta_\alpha = 10°$ and $\theta_d = -10°$, support the exclusion of complex form factors.
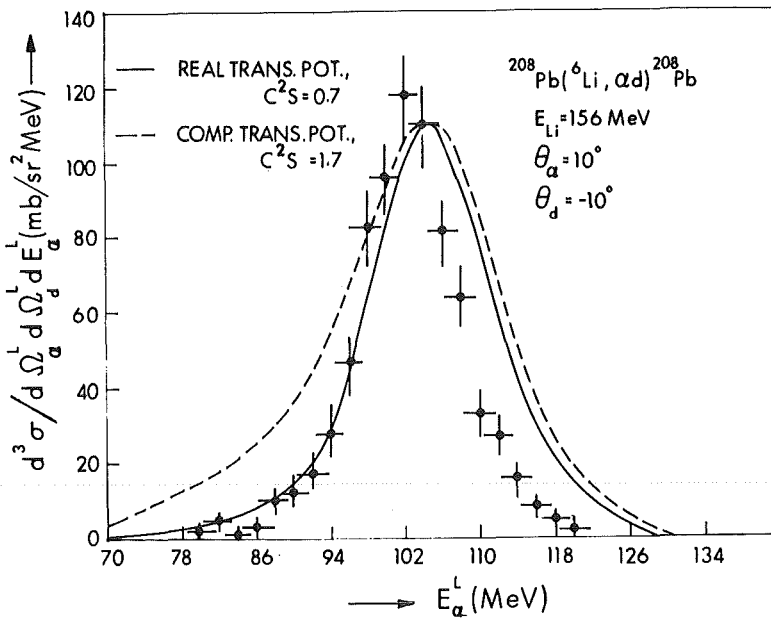

Fig. 9 Theoretical prior-form DWBA cross sections for break-up of 156 MeV 6Li colliding with 208Pb based on conventional transition potentials as compared to experimental results.

Fig. 9 presents results of calculations of the triple differential cross sections for real and complex form factors based on the potentials given in tab. 2. The real form factor yields not only a better description of the data, the normalization of the theoretical results to the experimental cross section at $E_\alpha^L = 104$ MeV results
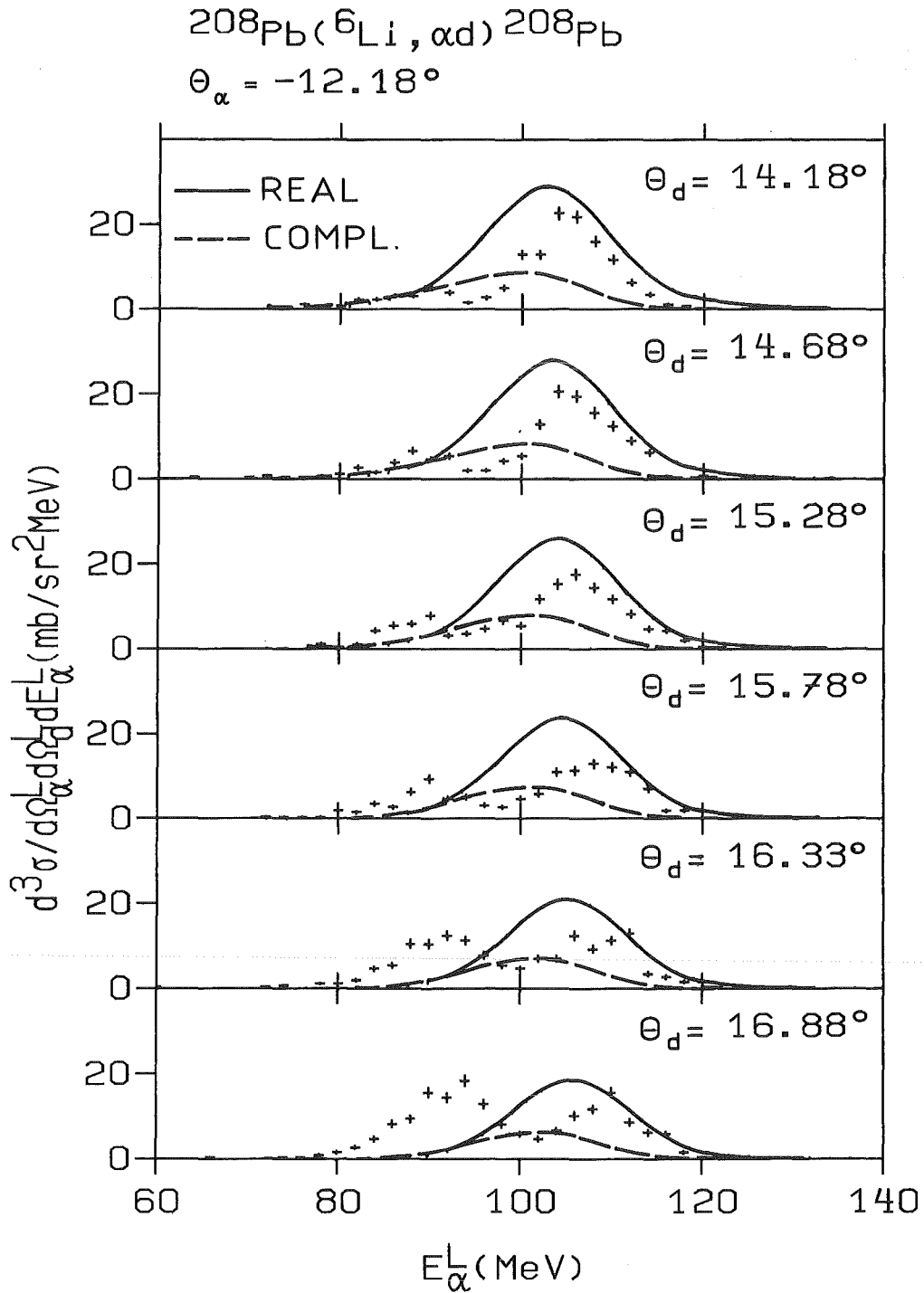
$^{208}Pb(^6Li, \alpha d)^{208}Pb$

$\Theta_\alpha = -12.18°$

REAL
COMPL.

$\Theta_d = 14.18°$

$\Theta_d = 14.68°$

$\Theta_d = 15.28°$

$\Theta_d = 15.78°$

$\Theta_d = 16.33°$

$\Theta_d = 16.88°$

$d^3\sigma/d\Omega_\alpha^L d\Omega_d^L dE_\alpha^L (mb/sr^2 MeV)$

$E_\alpha^L (MeV)$

Fig. 10a   Prior-form DWBA description of break-up of 156 MeV ^6Li incident on ^{208}Pb based on transition potentials from elastic fragment-target scattering ($C^2S = 0.7$).
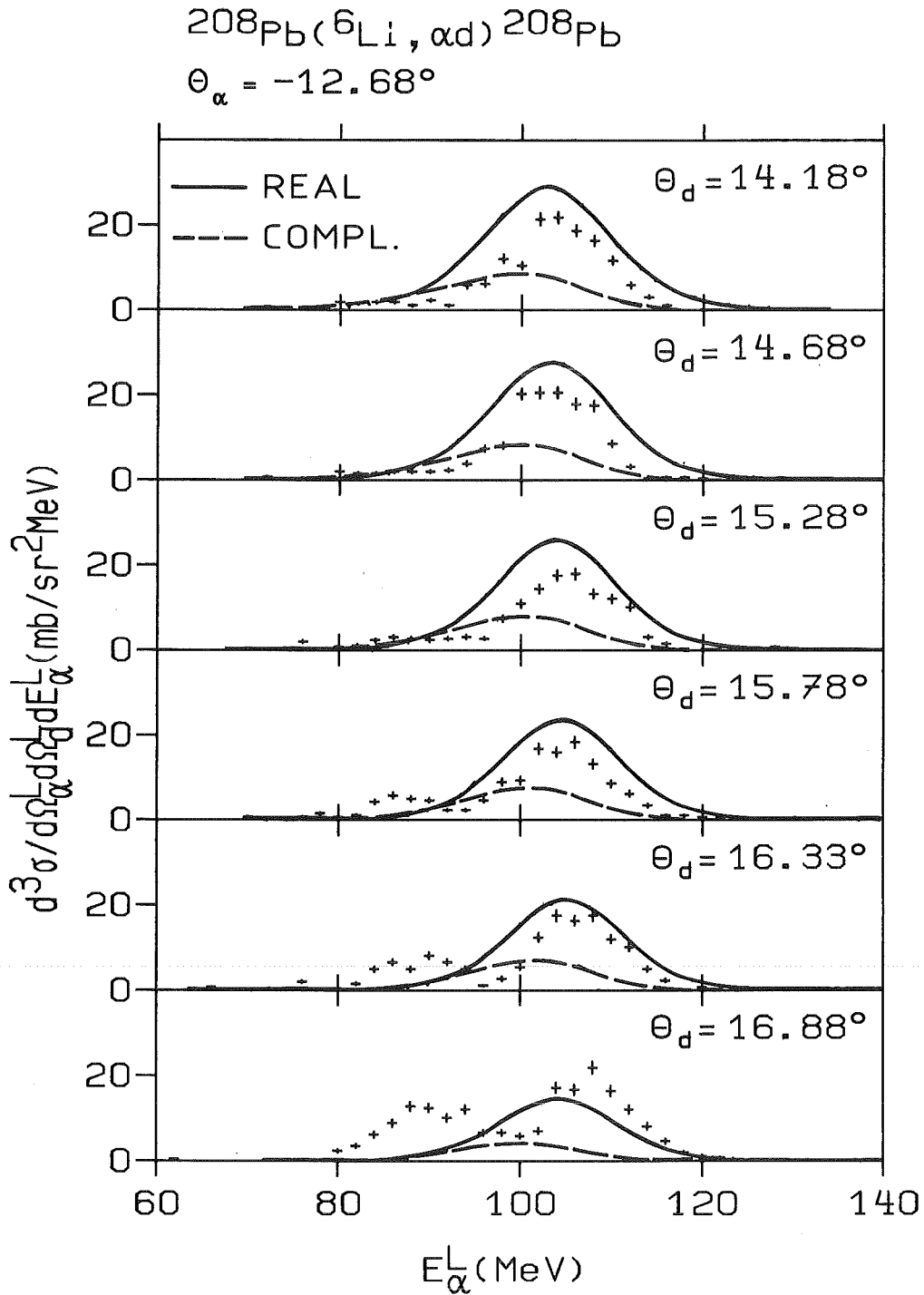
Fig. 10b Prior-form DWBA description of break-up of 156 MeV ^{6}Li incident on ^{208}Pb based on transition potentials from elastic fragment-target scattering (C^{2}S = 0.7).

in a value C2S = 0.7. This value is in good agreement with the value preferred in literature [23] and based on other information. We note the feature - similarily observed in a zero-range post-form DWBA description [11] of these data - that the peaks of the theoretical curves are slightly shifted to larger energies as compared to the data. But we remember (see fig. 5) that the exact peak position result from a delicate superposition of the two partial amplitudes of eq. 3.1.

The application to the analysis of the triple differential cross sections showing richer structures with double-peaked shapes (figs. 10a, b) reveals that the use of the conventional transition potentials fails to reproduce these features. However, we recall from fig. 6 that the prior-form treatment does provide such structures, though in a different angular range. Looking more closely, we find that the experimental minima always appear at $Q \approx 0.36$ fm^{-1}. The DWBA calculations when based on the elastic scattering potentials $U_{\alpha Pb}$ and U_{dPb} given in tab. 2 locate the dip at $Q \approx 0.59$ fm^{-1} (fig. 6). This finding has been tentatively associated[10] to the inadequacy of elastic (on-shell) scattering potentials to represent the fragment-target interactions inducing the break-up transition. Consequently modifying the potentials $U_{\alpha Pb}$ and U_{dPb} it has been shown that

$$^{208}Pb(^6Li, \alpha d)^{208}Pb$$
$$\Theta_\alpha = -10.00^\circ$$
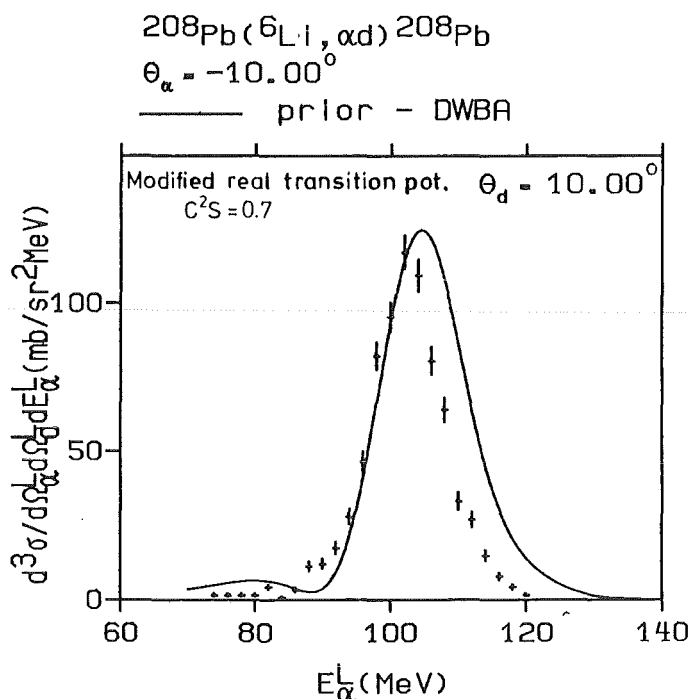$$\text{———— prior — DWBA}$$

Fig. 11 Theoretical prior-form DWBA cross sections for break-up of 156 MeV ^{6}Li colliding with ^{208}Pb : calculations with real form factors using the modified transition potentials.
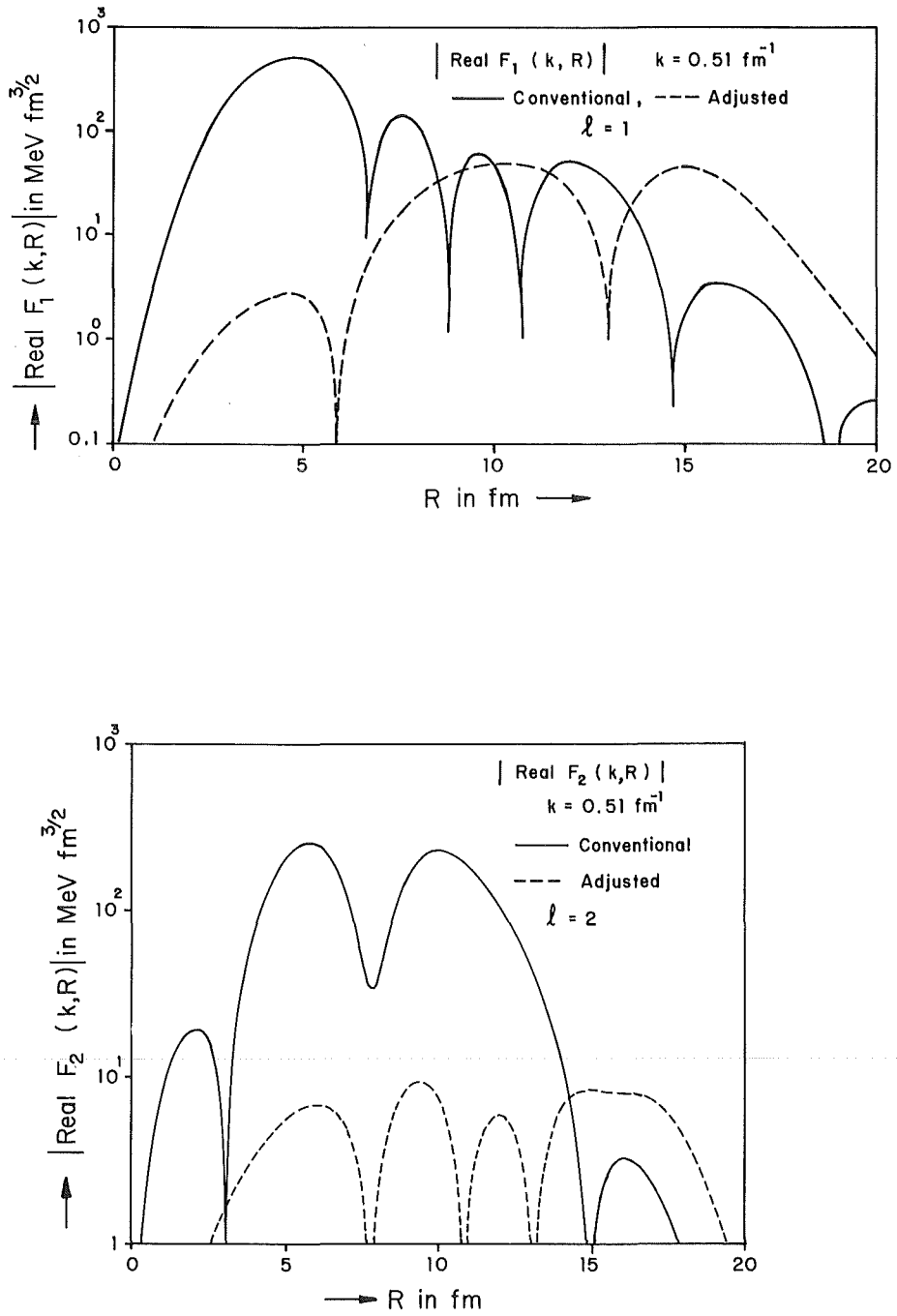
Fig. 12 The real dipole and quadrupole form factors calculated with the modified transition potentials as compared to those resulting from the elastic scattering potentials ($\ell = 1,2$ in fig. 1).

Tab. 4   Real transition potentials for the prior-form DWBA analysis of the
208Pb (6Li, ɑd) 208Pb elastic break-up.*

V [MeV]	a_v [fm]	r_v [fm]	J_v/A_pA_T [MeV·fm³]	Remark
-6.4	0.9	2.5	108	$U_{\alpha Pb}$
-4.0	0.8	1.8	52	U_{dPb}

*)   *The strengths of the transition potentials are ca. 8% smaller than the
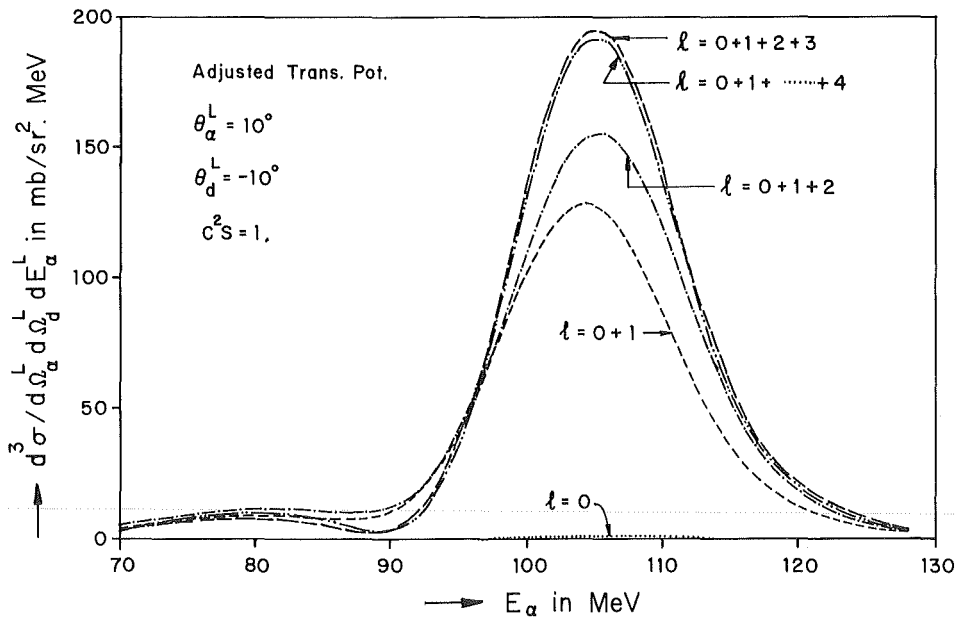preliminary values given in ref. 10.*

Fig. 13   Calcutated triple differential cross sections for elastic break-up of
156 MeV 6Li colliding with 208Pb resulting from adjusted transition
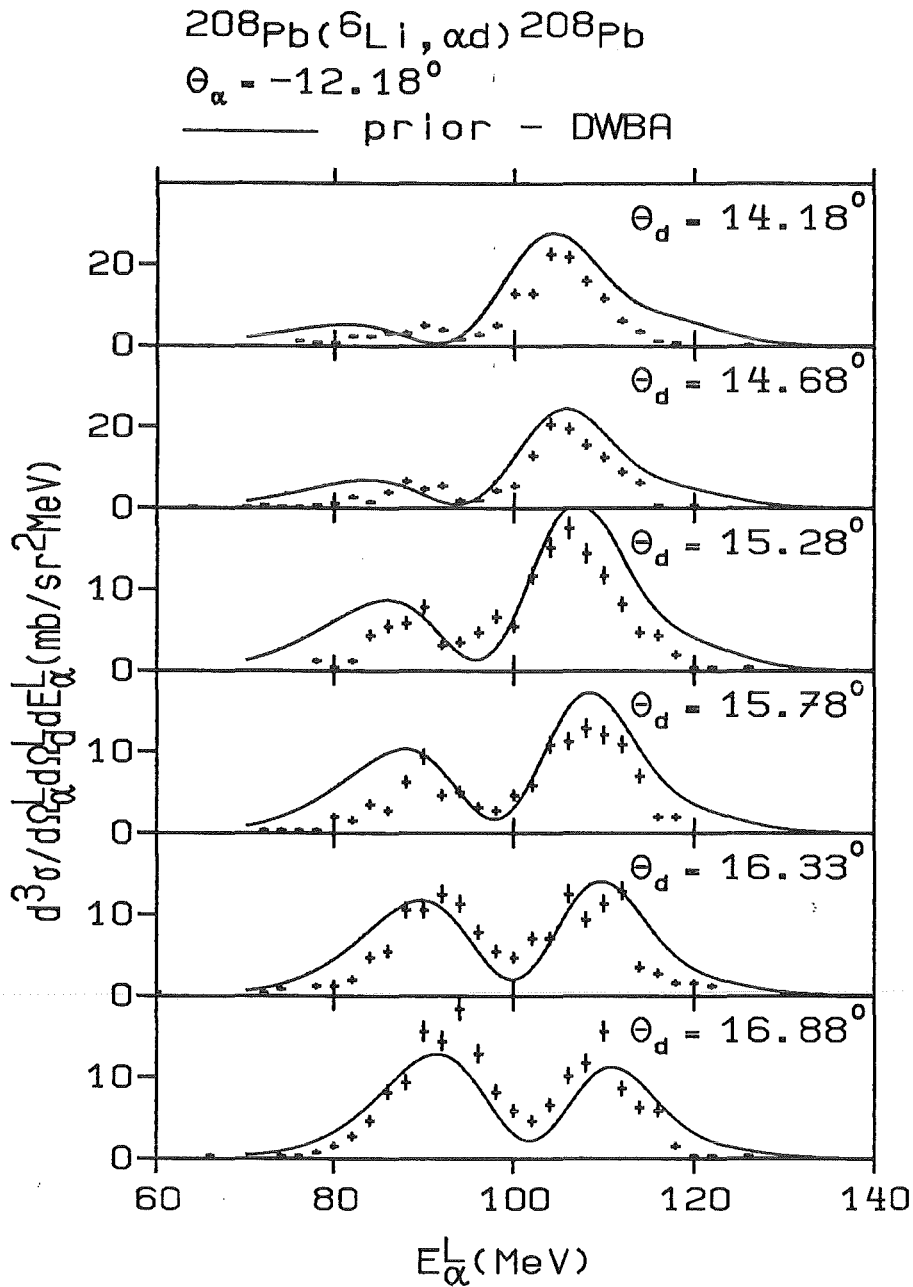potentials.

Fig. 14a   Prior-form DWBA description of break-up of 156 MeV ^{6}Li incident on
^{208}Pb based on transition potentials different from the optical potentials describing elastic fragment-target scattering.
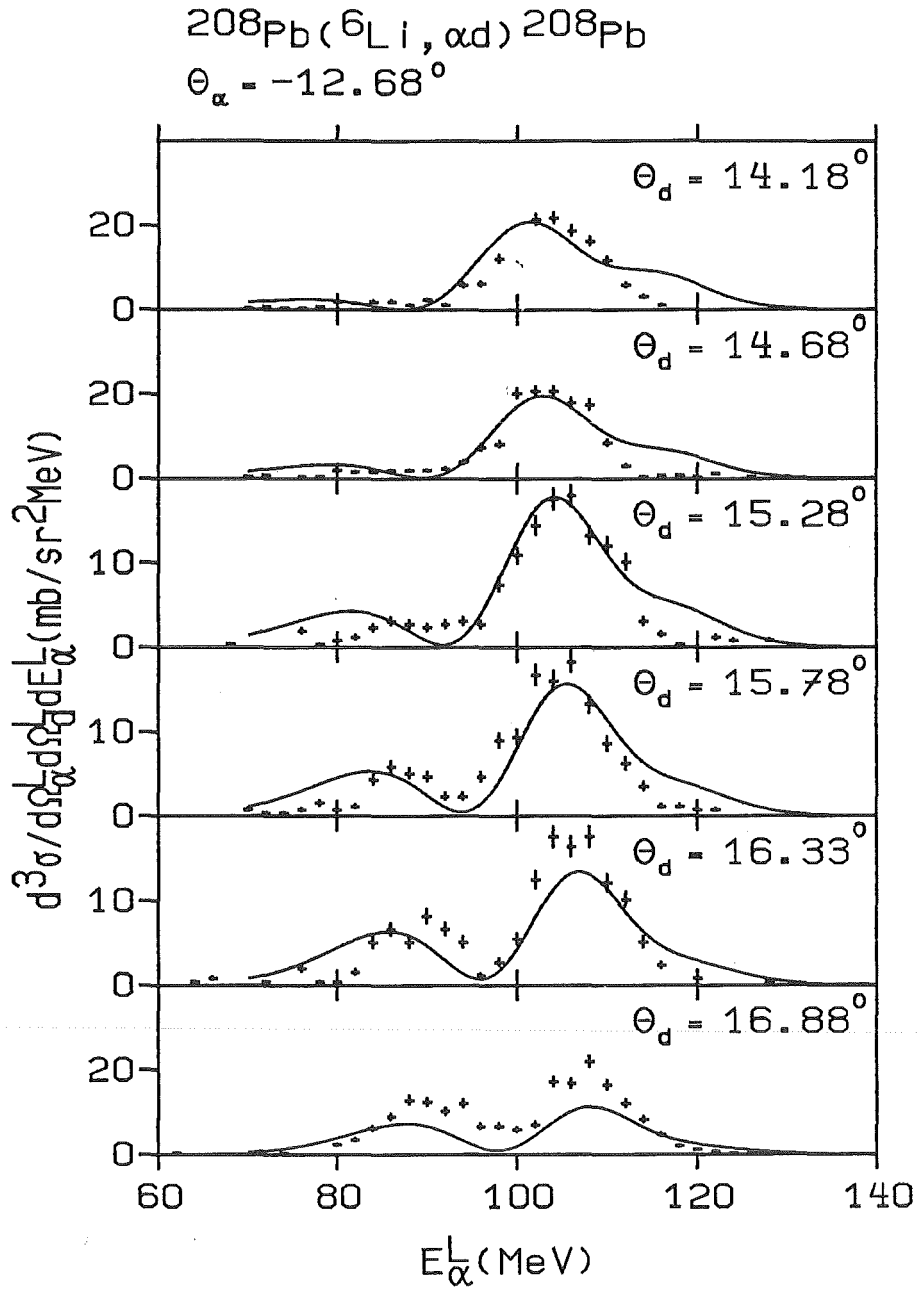
Fig. 14b Prior-form DWBA description of break-up of 156 MeV ^{6}Li incident on
208Pb based on transition potentials different from the optical poten-
tials describing elastic fragment-target scattering.

much shallower and spatially distinctly more extended transition potentials (tab. 4) approximately reproduce the data. We use these potentials, first repeating the calculation of the triple differential cross section for the case already shown in fig. 9. The result of fig. 11 demonstrates that the modified potentials are equivalent for the situation of smaller relative emission angles. This may be understood when considering the peripherial nature of the reaction by comparing the form factors calculated for the two different sets of transition potentials (fig. 12). Due to the strongly oscillating dipole form-factor for the conventional transition potentials the leading contribution comes from the quadrupole break-up. In contrast the dipole contribution is substantial for the adjusted transition potentials given in tab. 4. The quadrupole break-up contribution is correspondingly small in this case. This feature is shown in fig. 13 by the triple differential cross sections for the situation depicted earlier in fig. 3, but now recalculated with the adjusted transition potentials. Again sufficient convergence is achieved by summing up contributions up to $\ell = 4$. We would like to draw the attention also to fig. 2 where double-differential cross sections for the adjusted transition potentials are shown as solid bars. The application of these transition potentials (tab. 4) to the data covering the critical region (around $Q \simeq 0.36$ fm^{-1}) demonstrate that they are also able to account for the experimental observations there. For demonstration (fig. 14) a set of experimentally studied cases has been selected which has been already considered elsewhere[11] within the so-called diffractive dissociation approach and in figs. 10a and 10b above. All further experimental data which we have examined with these modified potentials are fairly well reproduced by the calculations though minor deficiencies, in particular in the angular dependence are seen. Due to the necessary amount of computer time we did not apply a consistent procedure using an automatic fitting routine for searching the χ^2- minimum. In so far the fits can potentially be further improved, thus removing small inconsistencies and with exploring possible ambiguities. Nevertheless the present results demonstrate that break-up studies extended to larger relative energies of the fragments are able to reveal interesting features of the effective fragment-target interactions.

5. CONCLUDING REMARKS

Recently published [9-11] triple differential cross sections for elastic break-up of 156 MeV ^{6}Li projectiles incident on ^{208}Pb, measured for large relative asymptotic energies of the fragments (> 5 MeV) and showing conspicuously structured shapes, have been analysed in the frame of the prior-form DWBA break-up approach. Coulomb break-up has been neglected for the considered cases. The

quadrupole mode is found to be dominant to nuclear break-up of $^6Li \rightarrow \alpha + d$ though additionally higher multipole components up to $\ell = 4$ coherently contribute with smaller effects if conventional transition potentials are used. Various sensitivities, in particular to the transition potentials are explored. In applying to the data the observed structures are found to reflect the structure of the amplitudes of the fragment-target (off-shell) scattering. Adjusting the transition potentials in such a way that the transition amplitudes cross a minimum in the considered range of momentum transfer leads to a successful description of the data with the other ingredients (the spectroscopic factor, e.g.) fixed in a reasonable way.

REFERENCES

1. T. Udagawa, T. Tamura, T. Shimoda, H. Fröhlich, M. Ishihara and K. Nagatani
   T. Udagawa and T. Tamura, Lecture presented at the RCNP-KIKUCHI Summer School on Nuclear Physics, Osaka, Japan, May 19 - 23, 1980

2. G. Baur, Proc. of the Daresbury Study Weekend on Topics in Heavy Ion Reactions, Daresbury, England, October 4 - 5, 1980 - DL/NUC/R21, eds. A.K. Dhar, J.S. Lilley and M.A. Nagarajan, SERC-Daresbury Laboratory 1981
   A. Budzanowski, Proc. 3rd Adriatic Europhys. Conf. on Dynamics of Heavy Ion Collisions, Hvar, Yugoslavia, May 25 - 31, 1981

3. G. Baur and D. Trautmann, Phys. Rep. C 25 (1976) 293
   G. Baur, F. Rösel, D. Trautmann and R. Shyam, Phys. Rev. C 111 (1984) 333

4. F. Rybicki and N. Austern, Phys. Rev. C 6 (1972) 1525
   E.M. Henley and D.U.L. Yu, Phys. Rev. 133 B (1964) 1445

5. N. Austern, Phys. Rev. C 30 (1984) 1130

6. R. Shyam and M.A. Nagarajan, Ann. Phys.(New York) 163 (1985) 265

7. E.M. Henley and C.E. Lacy, Phys. Rev. 160 (1967) 835

8. D.K. Srivastava and H. Rebel, Proc. 4th Internat. Conf. on Nuclear Reaction Mechanisms Varenna, Italy, June 10 - 15, 1985, ed. E. Gadioli, Ricerca Scientifica ed I Educazione Permanente, University of Milano, Suppl. No. 46 (1985) p. 86

9. N. Heide, H. Rebel, V. Corcalciuc and D.K. Srivastava, Rev. Roum. Physique (in press)

10. N. Heide, D.K. Srivastava and H. Rebel, submitted to Phys. Rev. Lett.

11. N. Heide, H. Rebel, V. Corcalciuc, H.J. Gils, H. Jelitto, J. Kiener, J. Wentz, S. Zagromski and D.K. Srivastava, submitted to Nucl. Phys. A KfK-Report 4564 (1989) ISSN 0303 - 4003

12. A.G. Sitenko, M.V. Evlanov, A.D. Polozov and A.M. Sokolov, Sov. Nucl. Phys. 45 (1987) 465

13. D.K. Srivastava, D.N. Basu and H. Rebel, Phys. Rev. C38 (1988) 2148

14. J. Cook, H.J. Gils, H. Rebel, Z. Majka and H. Klewe-Nebenius Nucl. Phys. A388 (1982)173

15. H.J. Gils, H. Rebel, J. Buschmann, H. Klewe-Nebenius, G.P. Nowicki and W. Nowatzke, Z. Phys. A219 (1976) 53

16. G. Mairle, K.T. Knöpfle, H. Riedesel, G.J. Wagner, V. Bechtold and L. Friedrich, Nucl. Phys. A339 (1980) 61

17. N. Matsuoka, K. Hatanaka, T. Saito, T. Itahashi, K. Hosono, A. Shimizu, M. Kondo, F. Othani and O. Cynshi, Nucl. Phys. A 391 (1982) 357

18. A. Goto, H. Kamitsubo, N. Matsuoka and M. Sakaguchi, Nucl. Phys. A444 (1985) 248

19. Y. Sakuragi, M. Yahiro and M. Kamimura, Prog. Theor. Phys. Suppl. 89 (1986) 136

20. D.K. Srivastava, D.N. Basu and H. Rebel, Nucl. Phys. A485 (1988) 221

21. E.H.L. Aarts, R.A.R.L. Malfliet, R.J. de Meijer and S. van der Werf, Nucl. Phys. A425 (1984) 23

22. N. Heide, V. Corcalciuc, H.J. Gils, H. Rebel, S. Zagromski, D.K. Srivastava and C. Samanta, Proc. XXV Int. Winter Meeting on Nucl. Physics, Bormio, Italy Jan. 19-24, 1987, ed. I. Iori, Ricerca Scientifica ed Educazione Permanente, University Milano, Suppl. N. 56 (1987) p. 436
N. Heide, KfK-Report 4451 (1989) ISSN 0303-4003

23. R.G. Lovas, A.T. Kruppa, R. Beck and F. Dickmann
Nucl. Phys. A474 (1987) 451

24. C.M. Vincent, Phys. Rev. 175 (1968) 1309

25. M. Gell-Mann and M.L. Goldberger, Phys. Rev. 91 (1953) 398

26. R. Huby and J.R. Mines, Rev. Mod. Phys. 37 (1965) 406

27. D.K. Srivastava and H. Rebel, Phys. Rev. C33 (1986) 1221

28. N. Austern, private communication

29. I.J. Thompson and M.A. Nagarajan, Phys. Lett 123B (1983) 379

30. D.K. Srivastava, Lectures presented at the XVII th Int. Summer School of Nuclear Physics, Mikolajki, Poland, Sept. 1985 – KfK - Report 4007 (1985) – ISSN 0303-4003

31. G.H. Rawitscher, Phys. Rev. C9 (1971) 2210

32. Y. Sakuragi, M. Yahiro and M. Kamimura, Prog.Theoret. Phys. 70 (1983) 1047

APPENDIX

FORMULATION OF POST- AND PRIOR-FORM BREAK-UP DWBA APPROACHES

A three body model describing the break-up process

$$a + A \rightarrow b + x + A$$

is characterized by the Hamiltonian

$$H = T_b + T_x + U_{bA}(r_b) + U_{xA}(r_x) + U_{bx}(r) \tag{A.1}$$

where T_b and T_x denote the kinetic energies, U_{bA}, U_{xA} the optical potential) interactions of the break-up fragments with the target (A), and U_{bx} the interaction binding b and x in the projectile a with the ground state wave function $\phi_a(r)$, which appears as a stationary solution of the initial state Hamiltonian

$$H_i = T_b + T_x + U_{bx} \quad . \tag{A.2a}$$

The formulation of the transition matrix depends on the decomposition of the Hamiltonian (eq. A.1) into an unperturbed and a perturbed part. Neglecting the interaction U_{bx} the final states are generated by

$$H_f = T_b + T_x \tag{A.2b}$$

and the residual interaction is given by

$$V_f = H - H_f = U_{bA} + U_{xA} + U_{bx} \quad . \tag{A.2c}$$

The exact expression [24] for the post-form T-matrix results as

$$T_{post} = < e^{ik_b \cdot r_b} e^{ik_x \cdot r_x} | U_{bA} + U_{xA} + U_{bx} | \psi_i^{(+)} > \quad . \tag{A.3a}$$

The equivalent prior form representation is

$$T_{prior} = < \psi_f^{(-)} | U_{bA} + U_{xA} | e^{ik_a \cdot R} \phi_a(r) > \quad . \tag{A.3b}$$

These expressions involve the exact solutions $\psi_f^{(-)}$, $\psi_i^{(+)}$ of the full Hamiltonian (eq. A.1) with appropriate boundary conditions.

Using the Gell-Mann-Goldberger relation [25] to distort the plane wave in eq. A.3a and eq. A.3b by an (auxiliary) interaction potential $U_{bA} + U_{xA}$ and U_{aA} (R), respectively - the latter acting on the center-of-mass of the projectile (R) - the transition matrices are rewritten as

$$T_{post} = < \chi_b^{(-)}(r_b) \chi_x^{(-)}(r_x) | U_{bx} | \psi_i^{(+)} > \tag{A.4a}$$

$$T_{prior} = \langle \psi_f^{(-)} \mid U_{bA} + U_{xA} - U_{aA} \mid \chi_a^{(+)}(R) \phi(r) \rangle \quad . \tag{A.4b}$$

The distorted waves $\chi_a^{(+)}(R)$ and $\chi_b^{(-)}(r_b) \cdot \chi_x^{(-)}(r_x)$ describe the motion of the particles under the influence of the potentials U_{aA} and $(U_{bA} + U_{xA})$ in the entrance and the exit channels, respectively. The expressions (eq. A.4a and eq. A.4b) are the starting point for approximate treatments of the transition matrices.

Invoking the distorted wave Born approximation the DWBA transition matrix used in Baur's approach [3]

$$T_{post}(DWBA) = \langle \chi_b^{(-)} \chi_x^{(-)} \mid U_{bx} \mid \chi_a^{(+)} \phi_a \rangle \tag{A.5a}$$

is obtained by replacing

$$\psi_i^{(+)} \simeq \chi_a^{(+)} \phi_a \tag{A.5b}$$

Similarly, the equivalent [27] prior form (used by Srivastava and Rebel [8])

$$T_{prior}(DWBA) = \langle \chi_b^{(-)} \chi_x^{(-)} \mid U_{bA} + U_{xA} - U_{aA} \mid \chi_a^{(+)} \phi_a \rangle \tag{A.6a}$$

results from the approximation

$$\psi_f^{(-)} \simeq \chi_b^{(-)} \chi_x^{(-)} \quad . \tag{A.6b}$$

Calculations of break-up cross sections based on eq. A.5a and eq. A.6a provide reasonable results in cases where the relative energies of the fragments are sufficiently large, i.e. when the final state interaction is negligible.

At lower relative energies, however the increased importance of the interaction of the fragments in the final state has to be taken into account. Therefore, the final state in the transition matrix is better represented as solution of the final state Hamiltonian

$$\tilde{H}_f = T_b + T_x + U_{bx} \quad . \tag{A.7a}$$

Thus, the residual interaction to be used in the post form

$$\tilde{V}_f = H - H_f = U_{bA} + U_{xA} \tag{A.7b}$$

is identical to that of the prior form of the transition matrix. We have

$$T_{post}^{FSI} = \langle e^{iK_f \cdot R} \phi_k^{(-)}(r) \mid U_{bA} + U_{xA} \mid \psi_i^{(+)} \rangle \tag{A.8a}$$

and

$$T_{prior}^{FSI} = \langle \psi_f^{(-)} \mid U_{bA} + U_{xA} \mid e^{iK_i \cdot R} \phi_a(r) \rangle \tag{A.8b}$$

where the supercript ' FSI ' indicates the inclusion of final state interactions and

$$K_f = k_b + k_x \qquad \text{(A.9a)}$$

$$k = \frac{m_b}{m_a} k_x - \frac{m_x}{m_a} k_b \qquad \text{(A.9b)}$$

We note that we can also obtain T_{post}^{FSI} (eq. A.8a) as an exact expression [27], when U_{bx} is reduced in T_{post} (eq. A.3a) by use of the Gell-Mann-Goldberger-relation. The DWBA approximation of $\psi_i^{(+)}$ (eq. A.6b) leads to

$$T_{post}^{SrR} (DWBA) = < e^{i K_f \cdot R} \phi_k^{(-)} | U_{bA} + U_{xA} | \chi_a^{(+)} \phi_a > \qquad \text{(A.10)}$$

The difference of the formally equivalent expression (eq. A.4a and A.8a) reflects just the transition from H_f and V_f (eqs. A.2b and A.2c) to $\bar{H}_f$ and $\bar{V}_f$ (eqs. A.7a and A.7b), respectively, just emphasizing the situation, where U_{bx} acts significantly in the final state, i.e. at small relative energies. The above expression (eq. A.10) is consistent with the finding of Austern [5] that the appropriate distorting potential for the exit channel centre of-mass-motion tends to zero as k→0. if the DWBA approximation (eq. A.5b) has to hold. At larger values of k the expression (eq. A.10) may be less accurate [28] as the representation of the final state does not account for the distortion of motion of b and x (arguing, that eq. A.10 includes the distortion for the exit channel only up to first oder).

Considering again the transition matrices T_{post}^{FSI} (eq. A.8a) and T_{prior}^{FSI} (eq. A.8b), these expressions can be reduced by introducing a potential U

$$T_{post}^{FSI} = < \chi_U^{(-)} \phi_k^{(-)} | U_{bA} + U_{xA} - U | \psi_i^{(+)} > \qquad \text{(A.11a)}$$

$$T_{prior}^{FSI} = < \psi_f^{(-)} | U_{ba} + U_{xA} - U | \chi_U^{(+)} \phi_a > \qquad \text{(A.11b)}$$

Applying the DWBA approximation (corresponding to eq. A.5b) Rybicki and Austern identified U with the *entrance channel* optical potential U_{aA} for distorting the centre of mass motion of the exit channel.

$$T_{post}^{RyA} (DWBA) = < \chi_{a*}^{(-)} \phi_k^{(-)} | U_{bA} + U_{xA} - U_{aA} | \chi_a^{(+)} \phi_a > \equiv T_{prior}^{RyA} (DWBA) \qquad \text{(A.12)}$$

As U_{aA} (R) only acts on $\chi_a^{(\pm)}$, the term involving U_{aA} actually drops off due to the orthogonality of ϕ_k and ϕ_a.

$$H = T_b + T_x + U_{bA} + U_{xA} + U_{bx}$$
$$H_i = T_b + T_x + U_{bx}$$

Quasi free break-up : $H_f = T_b + T_x$

Sequential break-up : $H_f = T_b + T_x + U_{bx}$

$$T_{post} = \langle e^{i\vec{k_b}\vec{r_b}} e^{i\vec{k_x}\vec{r_x}} | U_{bA} + U_{xA} + U_{bx} | \psi_i^{(+)} \rangle$$

$$T_{prior} = \langle \psi_f^{(-)} | U_{bA} + U_{xA} | e^{i\vec{k_a}\vec{R}} \phi_a \rangle$$

(U_x)

$$T_{post}^{FSI} = \langle e^{i\vec{K}\vec{R}} \phi_k^{(-)} | U_{bA} + U_{xA} | \psi_i^{(+)} \rangle$$

$$T_{prior}^{FSI} = \langle \psi_f^{(-)} | U_{bA} + U_{xA} | e^{i\vec{k_a}\vec{R}} \phi_a \rangle$$

$$T_{post} = \langle \chi_b^{(-)} \chi_x^{(-)} | U_{bx} | \psi_i^{(+)} \rangle$$

$$T_{prior} = \langle \psi_f^{(-)} | U_{bA} + U_{xA} - U_{aA} | \chi_a^{(+)} \phi_a \rangle$$

$$T_{post}^{FSI} = \langle \chi_{a*}^{(-)} \phi_k^{(-)} | U_{bA} + U_{xA} - U_{aA} | \psi_i^{(+)} \rangle$$

$$T_{prior}^{FSI} = \langle \psi_f^{(-)} | U_{bA} + U_{xA} - U_{aA} | \chi_a^{(+)} \phi_a \rangle$$

$$\boxed{D \ W \ B \ A}$$

$$T_{post} (DWBA) = \langle \chi_b^{(-)} \chi_x^{(-)} | U_{bx} | \chi_a^{(+)} \phi_a \rangle$$

$$T_{prior} (DWBA) = \langle \chi_b^{(-)} \chi_x^{(-)} | U_{bA} + U_{xA} - U_{aA} | \chi_a^{(+)} \phi_a \rangle$$

$$\left.\begin{array}{l} T_{post}^{RyA} \ (DWBA) \\[4pt] T_{prior}^{RyA} \ (DWBA) \end{array}\right\} = \langle \chi_{a*}^{(-)} \phi_k^{(-)} | U_{bA} + U_{xA} - U_{aA} | \chi_a^{(+)} \phi_a \rangle$$

$$T_{post}^{SrR} (DWBA) = \langle e^{i\vec{K}\vec{R}} \phi_k^{(-)} | U_{bx} + U_{xA} | \chi_a^{(+)} \phi_a \rangle$$

Fig. A1 Genealogy of prevailing post- and prior-form representations
of the break-up transition amplitude.

Summarizing the discussion of the current approaches (Fig. A1), we realize that the prevailing post-form DWBA theories *) essentially neglect the final state interaction between the fragments of the broken-up projectile, but they include the distortion of their motion in the field of the residual nucleus rather accurately. In contrast, the prior-form theories include the final state interaction accurately [29], but they introduce a somewhat inaccurate distortion by using the entrance channel optical potential itself to distort the centre of mass motion of the fragments. Tolerating the latter inaccuracy would immediately imply [30] that the two types of DWBA theories are valid respectively in the regions of large and small relative energies of the emerging fragments.

Even though not quite successful the current prior form theory has the specific advantage that for large relative momenta, ϕ_k approximates a plane wave due to the weakness of of U_{bx} and tends to describe the case of a neglected final state interaction (like the post-form approach). This indicates that the frame-work of the prior formulation should serve as a useful base on which a theory applicable over a wider range of relative energies may be built. It is interesting to note that coupled channel treatments [31,32] of the problem in fact start by expanding (in eqn. A.11a)

$$\psi^{(+)} = \chi_a^{(+)} \, \phi_a + \int d\mathbf{k} \, \phi_k \cdot \chi_{K_f}^{(+)} \tag{A.12}$$

and solving for the correction term.

---

*) The terminology has become conventional [5] to call the expressions (eqs. A.4a and A.5a) the "post"-form, and the expressions (eqs. A.11a, A.11b and A.12) the "prior"-form, even if there is no post-prior equivalence between eqs. A.5a and A.12, since they are based on different representations of the exit channel.